Asian Journal of Chemistry; Vol. 33, No. 2 (2021), 471-483

ASIAN JOURNAL OF CHEMISTRY

https://doi.org/10.14233/ajchem.2021.23021

Sorption of Chromium(VI), Cadmium(II) Ions and Methylene Blue Dye by Pristine, Defatted and Carbonized *Nigella sativa* L. Seeds from Aqueous Solution

PATIENCE MAPULE THABEDE*, NTAOTE DAVID SHOOTO* and ELIAZER BOBBY NAIDOO

Applied Chemistry and Nano Science Laboratory, Department of Chemistry, Vaal University of Technology P.O. Box X021, Vanderbjlpark 1900, South Africa

*Corresponding authors: E-mail: mapulepseabelo@gmail.com; ntaotes@vut.ac.za

Received: 12 October 2020; *Accepted*: 4 December 2020; *Published online*: 15 January 2021; AJC-20237

Present study reports on the sorption study of chromium(VI), cadmium(II) ions and methylene blue dye by pristine, defatted and carbonized *Nigella sativa* L. seeds from aqueous solution. The removal of oil from pristine *Nigella sativa* L. (PNS) seeds was carried out by defatting the *Nigella sativa* with acetone and *N,N*-dimethylformamide and then labelled ANS and DNS, respectively. Thereafter the defatted ANS and DNS adsorbents were carbonized at 600 ºC for 2 h under nitrogen and labelled as CANS and CDNS. The results of pristine, defatted and carbonized seeds were compared. The removal of Cr(VI), Cd(II) and methylene blue dye from aqueous solutions was investigated by varying adsorbate concentration, solution pH, reaction contact time and temperature of the solution. The SEM images indicated that the surface morphology of PNS was irregular, whilst ANS and DNS had pores and cavities. CANS and CDNS was heterogeneous and had pores and cavities. FTIR spectroscopy showed that the adsorbents surfaces had bands that indicated a lot of oxygen containing groups. The pH of the solution had an influence on the removal uptake of Cr(VI), Cd(II) and methylene blue. The sorption of Cr(VI) decreased when pH of the solution was increased due to different speciation of Cr(VI) ions whilst the removal of Cd(II) and methylene blue increased when solution pH was increased. Pseudo first order kinetic model well described the adsorption of Cr(VI), Cd(II) and methylene blue onto PNS. On the other hand, the kinetic data for ANS, CANS, DNS and CDNS was well described by pseudo second order. Furthermore, the removal mechanism onto PNS and ANS was better described by Freundlich multilayer model. The CANS, DNS and CDNS fitted Langmuir monolayer model. Thermodynamic parameters indicated that the sorption processes of Cr(VI), Cd(II) and methylene blue was endothermic and effective at high temperatures for all adsorbents. The ΔS° and ΔH° had positive values this confirmed that the sorption of Cr(VI), Cd(II) and methylene blue onto all adsorbents was random and endothermic, respectively. The values of ΔG° confirmed that the sorption of Cr(VI), Cd(II) and methylene blue on all adsorbents was spontaneous and predominated by physical adsorption process. The CANS had highest adsorption capacity of 99.82 mg/g for methylene blue, 96.89 mg/g for Cd(II) and 87.44 mg/g for Cr(VI) followed by CDNS with 93.90, 73.91 and 65.38 mg/g for methylene blue, Cd(II) and Cr(VI), respectively. The ANS capacities were 58.44, 45.28 and 48.96 mg/g whilst DNS capacities were 48.19, 32.69 and 34.65 mg/g for methylene blue, Cd(II) and Cr(VI), respectively. PNS had the lowest sorption capacities at 43.88, 36.01 and 19.84 mg/g for methylene blue, Cd(II) and Cr(VI), respectively.

Keywords: Chromium, Cadmium, Methylene blue, *Nigella sativa*, Pristine, Defatted, Adsorption.

INTRODUCTION

Activated carbon (AC) is a material that used in the industrial processes for purification of liquid and product separation [1]. Activated carbon is used as adsorbent for the removal of inorganic and organic pollutants in water, treatment of toxic compounds in medicine, as a material for storing hydrogen and many others [2]. Chemical and physical activation together with heating process is often used to produce carbon-based materials in order to enhance porous structure, improves surface area, improving rate of adsorption [3]. However, these materials are not easy to generate because they require high cost precursors [4]. Hence plant materials are used because they are abundant and sustainable resource that may provide oxygen containing groups which can easily interact with charged toxic pollutants from aqueous solution [5]. However, these materials need some modifications in order to get significant results for the removal of toxic ions and dyes [6].

Sorption of dyes and toxic metals onto solid surface is one of the most increasing methods for water treatment which is industrially favourable and environmentally friendly [7]. This method maybe be more effective, because the adsorbent could be prepared easily and can be effective for wide range of pollutants which in turn will be effective for the removal of toxic metal ions [8]. *Nigella sativa* L. is an annual vegetal spice belongs to the Ranunculacea family known as black cumin seed [9,10]. It is used for remedial purposes in the Asia, India, Parkistan, Turkey, Sourthen Europe and Africa [11,12]. Also, it has been traditionally used for the treatments related to respiratory health, intestinal health and stomach, liver and kidney function and immune system support. Other therapeutic effects include anti-inflammatory, antiallergic, analgesic, anticancer, antioxidants and antiviral [13-15]. Black cumin seeds contains appreciable amount of unsaturated especially polyunsaturated fatty acids which constitute the bulk of oil ranging from 48 to 70%, whilst monounsaturated (18-29%) and saturated fatty acids (12-25%) are in lesser amounts [10]. Fatty acids are reported to block the pores and in turn decreases the surface area of the biomaterials [10]. It is therefore, important to extract the oil from the *Nigella sativa* L. seeds before their application in wastewater treatment [16]. This process increases the cellulosic pore concentrations also, it increases the surface-active sites on the adsorbent material whereby functional groups such as -OH, -COO and -NH_2 can take part in the metal ion and dye binding [17,18]. Hence, the sorption of chromium Cr(VI), Cd(II) and methylene blue (MB) dye using pristine, defatted and carbonized *Nigella sativa* L. seeds is investigated.

Cr(VI) and Cd(II) ions are common toxins in wastewater resulting from industrial activities including paint manufacturing plants, textile manufacturing, petroleum refining, electroplating, paper, leather tanning, ceramic industries and other metal finishing industries [19]. On the other hand, methylene blue dye is found in effluent released from manufactures such as finishers, textile producers and dyers [20-22]. There are several health and negative environmental effects of methylene blue to human such as vomiting, chest pain, stomach pain, high fever, damages to central nervous systems cardiovascular and gastrointestinal [23]. Therefore, the removal of dyes from waste effluent becomes a global environmental issue because some dyes and their degradation products may be toxic also their treatment cannot depend on biodegradation alone [20,22].

Cr(VI) is one of the pollutants which has caught attention in the research field due to its toxicity. There are two types of stable chromium in nature [24] trivalent Cr(III) and hexavalent Cr(VI). Chromium(VI) has more toxic effects than Cr(III) to animals, humans and aquatic life due to its high solubility and mobility [25,26]. It causes lung cancer, damage the kidneys, gastric and liver in humans [27]. Therefore, it is important to remove Cr(VI) in water before is discharged into the environment, also because Cr(VI) is non-biodegradable and can stay for a long time in the environment. Cadmium(II) is one of the most toxic contaminants and found in agricultural soils and aquatic environments [28]. Health hazards associates with Cd(II) are toxicity and carcinogenic in nature and higher levels can cause hypertension, anaemia and damage to kidneys [29].

The adsorption of toxic metal ions and dye from the aqueous solutions using different low-cost defatted adsorbents have been conducted by many researchers [30-34]. Gilbert *et al.* [30] observed that the treatment of *Carica papaya* seeds with hexane gave the sorption capacity of 1666.67 mg/g for Pb^{2+} and 1000 mg/g for Cd^{2+}. Chandra *et al.* [18] treated alga with *n*-hexane and compared the raw alga with the defatted alga for the removal of methylene blue dye. The results showed that the maximum adsorption capacity for raw was 6.0 whilst the defatted alga was 7.73 mg/g and the specific surface area of raw, defatted was estimated to be 14.70, 18.94, $m^2 g^{-1}$, respectively. Kowanga *et al.* [31] mentioned that the treatment of moringa powder with hexane made the moringa to be an efficient biosorbent for removal of Pb(II) and Cu(II) from aqueous solution. Fontoura *et al.* [32] chemically treated microalgal biomass with a mixture of chloroform:methanol:water ratio for the removal of acid blue 161 dye. Their results showed that the maximum adsorbed amounts of AB-161 dye was 75.78 mg/g at 25 ºC. Shooto *et al.* [33] treated mucuna beans with acetone, methanol and dimethylformamide for the removal of Pb(II) ions and methylene blue dye from aqueous solution. Their findings revealed that the chemically treated adsorbents had higher adsorption capacity for methylene blue molecules than Pb(II) ions. The maximum capacities for Pb(II) with acetone, methanol and dimethylformamide were 18.94,16.15 and 17.60 mg/g, respectively whereas the results for methylene blue were 22.78, 24.56 and 23.89 mg/g. Therefore, chemical treatment of biomass material will not only modify the chemical composition of the material but may also improve the adsorption capacity due to formation of new functional group [34]. To the best of our knowledge, there is no study that has been conducted using defatted *Nigella sativa* L. to remove Cr(VI), Cd(II) ions and methylene blue dye in a system using pristine, defatted and carbonized *Nigella sativa* L. seeds. The system parameters such as initial concentration, reaction contact time, temperature of the solution and solution pH were varied.

EXPERIMENTAL

Analytical grade chemicals acetone (99.5%), cadmium acetate (99.99%), potassium dichromate, methylene blue dye (82%) and *N,N*-dimethylformamide were purchased from Sigma-Aldrich South Africa LTD. and unprocessed *Nigella sativa* L. seeds were procured at the health shop in Vanderbijlpark, South Africa.

Preparation of bioadsorbents

Preparation of pristine *Nigella sativa* seeds (PNS): *Nigella sativa* seeds were washed with distilled water to remove dust and debris materials. The washing was carried out several times. Thereafter, the seeds were dried in an oven at 40 ºC for 24 h. The dried seeds were then stored in a desiccator for cooling. Thereafter, grounded using a blender with steel blades. The powder was sieved and then labelled pristine *Nigella sativa* seeds (PNS).

Preparation of acetone *Nigella sativa* seeds (ANS): The method of preparing the adsorbents was adopted from Shooto *et al.* [35] with modifications. The PNS seeds (10 g) were added

to 100 mL of acetone under stirring on a magnetic stove using the magnetic stirrer bar at room temperature. After 1 h the resultant material was washed with distilled water to remove excess reagent and dried for 24 h at 50 ºC. The seeds were designated acetone treated *Nigella sativa* seeds (ANS).

Preparation of dimethylformamide *Nigella sativa* seeds (DNS): Pristine seeds (10 g) was mixed with 100 mL of DMF under stirring for 1 h. Then the material was isolated and rinsed in distilled water. The material was dried at 50 ºC for 24 h. The seeds were designated dimethylformamide treated *Nigella sativa* seeds (DNS).

Preparation of carbon-based acetone *Nigella sativa* seeds (CANS) and carbon-based dimethylformamide *Nigella sativa* seeds (CDNS): Treated seeds (10 g) were carbonized at 600 ºC for 2 h in a horizontal furnace under nitrogen thereafter, the furnace was allowed to cool off under nitrogen flow. The carbonized seeds were then designated carbonized acetone treated *Nigella sativa* seeds (CANS) and carbonized dimethylformamide treated *Nigella sativa* seeds (CDNS).

Adsorption experiments: The stock solutions of 100 mg/L for $K_2Cr_2O_7$, $Cd(CH_3COO)_2$ and methylene dye were prepared by dissolving 0.1 g in 1 L of distilled water, respectively. The solution pH effect was evaluated at pH 1, 3, 5, 7 and 9. The pH was adjusted by 0.1 M HCl for acidic medium and 0.1 M of NaOH for basic medium. A 20 mL of the adjusted solution was added to 0.1 g of adsorbent and equilibrated for 60 min. Effect of initial concentration was studied using standard solutions of 20, 40, 60, 80 and 100 mg/L and agitated for 120 min at 200 rpm. Contact time effect was tested intervals of 1, 5, 10, 15, 20, 30, 60, 90 and 120 min. The effect of temperature was studied at 298, 303, 313, 333 and 353 K by agitation at 200 rpm for 120 min. After agitation the mixtures were centrifuged at 5000 rpm for 5 min then decanted. The same procedure was followed for methylene blue dye. The determination of the point of zero charge (pH_{pzc}) for all adsorbents was determined using 1 M $NaNO_3$ concentration series of 100 mL. The solution pH 1 to 9 was adjusted by adding 0.1 M HCl for acidic medium and 0.1 M NaOH for basic medium. Then adjusted pH solutions were then added to 0.1 g of samples and agitated for 48 h at 200 rpm. After agitation the pH was measured. The final pH *versus* initial pH was plotted against pH values and the pHpzc was determined from the horizontal intersection point. The preparation method is shown in **Scheme-I**.

Data analysis: The amount of Cr(VI), Cd(II) ions and methylene blue dye onto the adsorbents was calculated by using equation:

$$q_e = \frac{(C_o - C_e)V}{m}$$

where C_o and C_e are the initial and final equilibrium concentrations (mg/L) of Cr(VI), Cd(II) and methylene blue in the solution, q_e is the amount adsorbed on the surface (mg/g), V is the volume of pollutants solution (L) and m is the mass of the adsorbent (g). Eqns. 1 and 2 were used to determine the removal capacity and the adsorption percentage, R (%) of Cr(VI), Cd(II) ions and methylene blue dye.

$$q_e = \frac{(C_o - C_e)V}{W} \quad (1)$$

$$R\ (\%) = \frac{(C_o - C_e)}{C_o} \times 100 \quad (2)$$

Adsorbents characterization: The biomaterials were characterized with scanning electron microscopy (SEM) taken on a Nova Nano SEM 200 from FEI operated at 10 kV in order to determine the surface morphology of the materials. Functional groups on the surface of the adsorbents were determined by Perkin-Elmer Fourier transformed infrared (FTIR) spectroscopy FTIR/FTNIR spectrometer, spectrum collected from 4000-400 cm^{-1}. The pH at point zero charge (pH_{PZC}) was determined by using the pH drift method where carbon adsorbents were added into 20 mL of 1 M $NaNO_3$ solutions with pH separately adjusted between 1 and 9. Adsorption capacity was determined using atomic adsorption spectroscopy (AAS) ASC 7000 from Shimadzu with auto sampler for determining the remaining Cr(VI) and Cd(II) in the solution. The methylene blue dye analyses were determined using ultraviolet-visible (UV-Vis) spectrophotometer, Perkin-Elmer Lambda 25 at 665

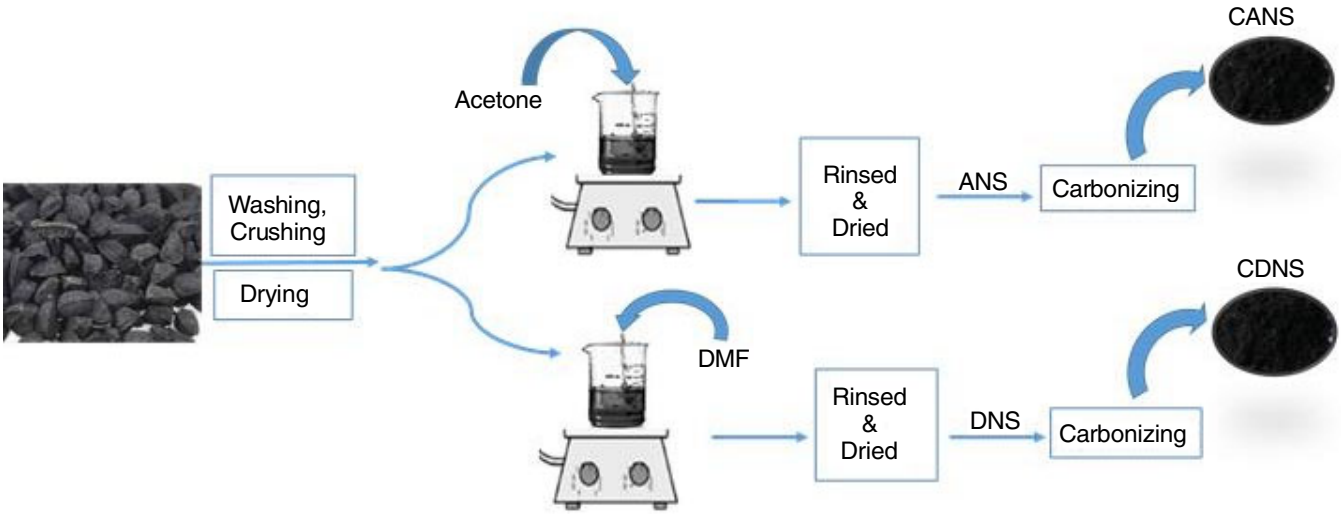

Scheme-I: Preparation of ANS, CANS, DNS and CDNS

nm, which collects spectra from 180 to 1100 nm UV and visible range with a slit of 1.0 and width of 0.1.

RESULTS AND DISCUSSION

SEM analysis: Fig. 1a-e show the morphology of the biosorbent surfaces determined by scanning electron microscopy. The PNS images (Fig. 1a) showed that the surface of adsorbent is composed of irregular morphology. Whilst, Fig. 1b displayed improved sphere-like morphology which was with porosity and cavities. Cavities might contributed to the biosorption of toxic ions and dyes [36]. The carbonized material for CANS in Fig. 1c displayed dense textural structure and spherical morphology. Fig. 1d-e the texture of the DNS and CDNS, respectively showed that the surface was irregular. Defatting with DMF and carbonization showed different surface texture which could be attributed to the fact that extraction of oil from biomass through solvent could lead to harsh effects of breaking the cell wall, which may cause such surface topology [32]. These characteristics are, therefore, estimated to increase the adsorption processes of Cd(VI), Cd(II) and methylene blue onto carbonized materials.

FTIR analysis: Fig. 2 represents the FTIR results of the adsorbents. Several peaks were identified which indicated the presence of various functional groups. A broad peak due to the free hydroxyl group (-OH) [37] was observed at 3304, 3291, 3296 and 3298 cm^{-1} for PNS, ANS, DNS and CDNS, respectively. The CANS did not display any noticeable peaks except the small peak at 1024 cm^{-1}. The small peak at 2999 cm^{-1} onto PNS was due to (-C-H) stretching in alkanes [2,38]. This peak shifted 3007, 3012 and 3010 cm^{-1} on ANS, DNS and CDNS, respectively. The two bands associated with methyl ($-CH_3$) and methylene ($-CH_2$) groups on PNS was observed at 2923 and 2848 cm^{-1} [39]. These peaks shifted to 2919 and 2849 cm^{-1} for ANS, whilst the peaks on DNS shifted to 2923 and 2844 cm^{-1} and for CDNS they were observed at 2919 and 2852 cm^{-1}. The absorbance peak at 1757 cm^{-1} onto PNS was identified as the vibration of the carbonyl group stretching (-C=O) [40,41]. This carbonyl peak on ANS shifted to 1744 cm^{-1}, whilst on DNS it shifted to 1740 and 1749 cm^{-1} in CDNS. The absorption peaks on PNS at 1647 and 1549 cm^{-1} were assigned to ν(-OH) vibration [42] and ν($-NH_2$) of the amide group, respectively [43]. However, on ANS the ν(-OH) peak shifted to 1649 and ν($-NH_2$) peak shifted to 1540 cm^{-1}. On the other hand, the amide peaks on DNS were observed at 1638 cm^{-1} for ν(-OH) group and 1545 cm^{-1} for the ν($-NH_2$) group. Meanwhile on CDNS the peaks were observed at 1642 and 1540 cm^{-1} for ν(-OH) and ν($-NH_2$) groups, respectively. The carboxyl ν(-COOH) stretching band was assigned at 1464, 1450, 1452 and 1451 cm^{-1} for PNS, ANS, DNS and CDNS, respectively [43,44]. The presence of CH_3 umbrella deformation vibrations were observed at 1376, 1368, 1365 and 1367 cm^{-1} on PNS, ANS, DNS and CDNS, respectively [45,46]. The bands at 1236, 1240, 1243 and 1248 cm^{-1} for PNS, ANS, DNS and CDNS were

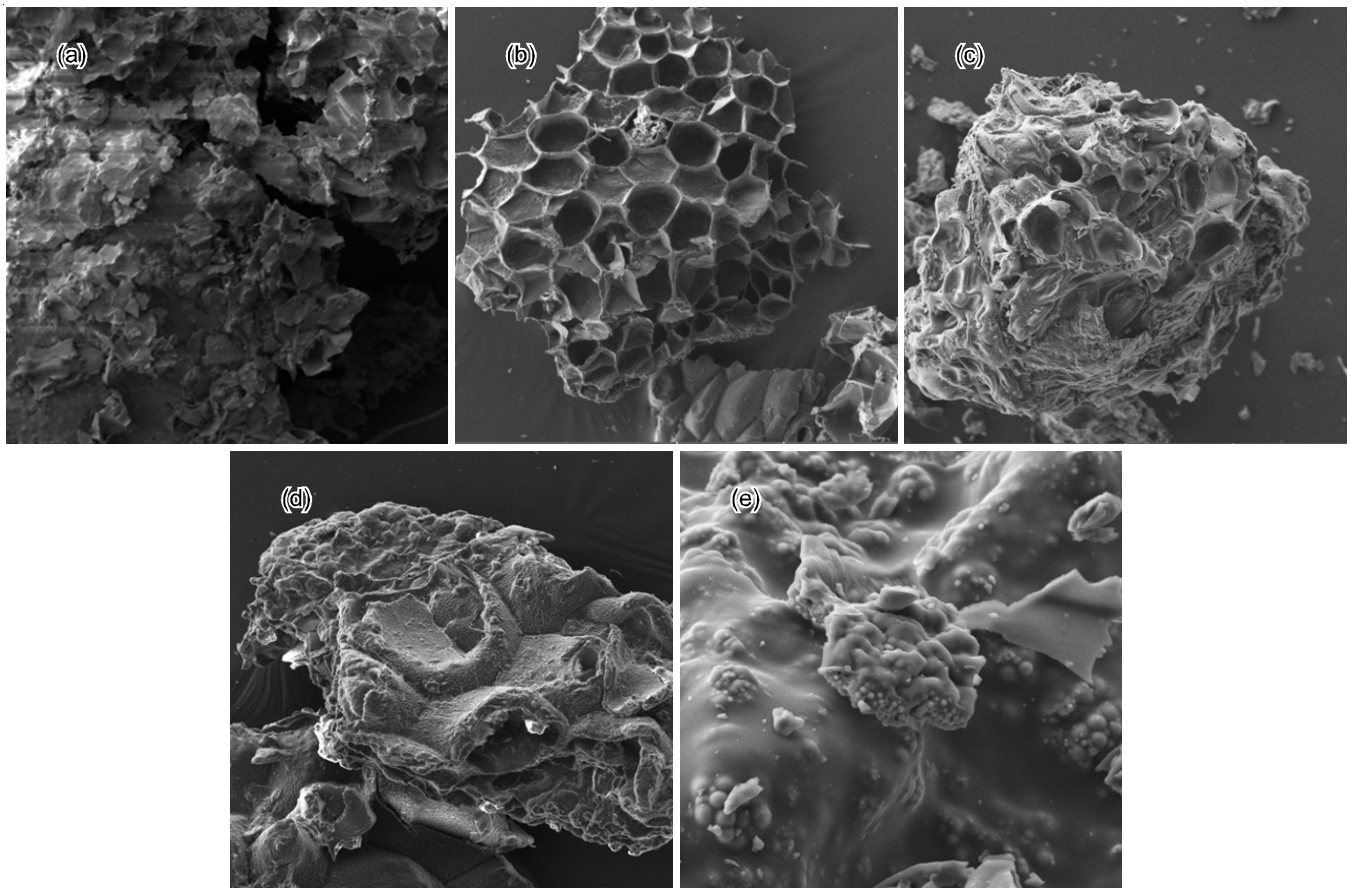

Fig. 1. SEM images of (a) PNS, (b) ANS, (c) CANS, (d) DNS and (e) CDNS

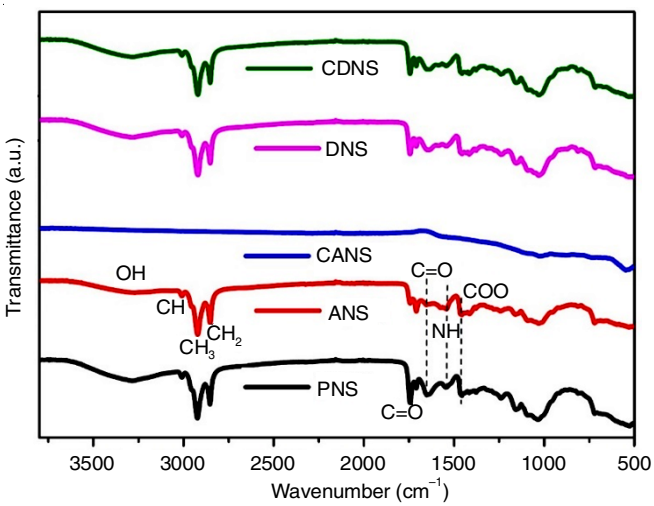

Fig. 2. FTIR spectrum of PNS, ANS, CANS, DNS and CDNS

related to O-H bending vibration, respectively [37]. The peak associated with the (-C-O-C) stretching vibrations of cellulose and hemicellulose material [13,47] was observed at 1169 cm^{-1} on PNS. After defatting the seeds, this peak shifted to 1165, 1154 and 1158 cm^{-1} on ANS, DNS and CDNS, respectively. The ν(-C-O) stretching vibration of carboxyl groups was observed at 1078, 1071, 1061 and 1068 cm^{-1} for PNS, ANS, DNS and CDNS, respectively [48]. The FTIR results showed that there were differences in the functional groups of the defatted and the pristine *Nigella sativa* seeds and that the seeds had negatively charged groups on their surface. The four spectra (PNS, ANS, DNS and CDNS) were similar with slight shifts in characteristic absorbance peaks. For each adsorbent, the shifts in transmission frequency proposed that there was interaction of various chemical treatments to the PNS seeds [42]. This suggests that the hydroxyl, carbonyl, amides and carboxyl groups were available for bonding [49].

Adsorption studies

pH and point zero charge of adsorbents: The zero-point charge (pH_{PZC}) of any solid is the pH at which the charge on the surface of the adsorbent is zero [50]. The pH_{PZC} values of PNS, ANS, ANS, DNS and CDNS are 5.81, 6.26, 5.65, 5.98 and 6.09, respectively. The pH_{PZC} values of all adsorbents were acidic but closer to neutral. The results showed that all the adsorbents had a similar behaviour therefore, it is expected that their pH pattern will be similar as well. The initial pH of adsorption is a very important parameter because it has an influence on the adsorption capacity [51]. It has the ability to change the ionization of the adsorbate, adsorbent surface load and the degree of the dissociation of the functional groups of adsorbate active sites [52]. The effect of pH was studied at 1, 3, 5, 7 and 9 as shown in Fig. 3a-e. The data showed that pH had an impact on adsorption performance for Cr(VI), Cd(II) and methylene blue. Fig. 3a-e showed that removal of Cr(VI) decreased as the pH increased, this was because at acidic pH value Cr(VI) exists as H_2CrO_4, $HCrO_4^-$, CrO_4^{2-} and $Cr_2O_7^{2-}$ [53]. At pH 2, the predominant species of Cr(VI) is $HCrO_4^-$ [54]. The high adsorption capacity of Cr(VI) at low pH was due to the electrostatic attraction of the protonated surface of the adsorbents [55]. The maximum adsorption capacity of Cr(VI) was obtained at pH 1 with maximum capacities ranging from highest to at 74.4, 48.9, 42.6, 34.7 and 20.7 mg/g on CANS, ANS, CDNS, DNS and PNS, respectively. Therefore, the adsorption capacity for Cr(VI) favoured acid conditions as compared basic conditions. Meanwhile, the removal of Cd(II) and methylene blue increased with the increased pH for all the adsorbents with low sorption at pH 1 and 3. This resulted

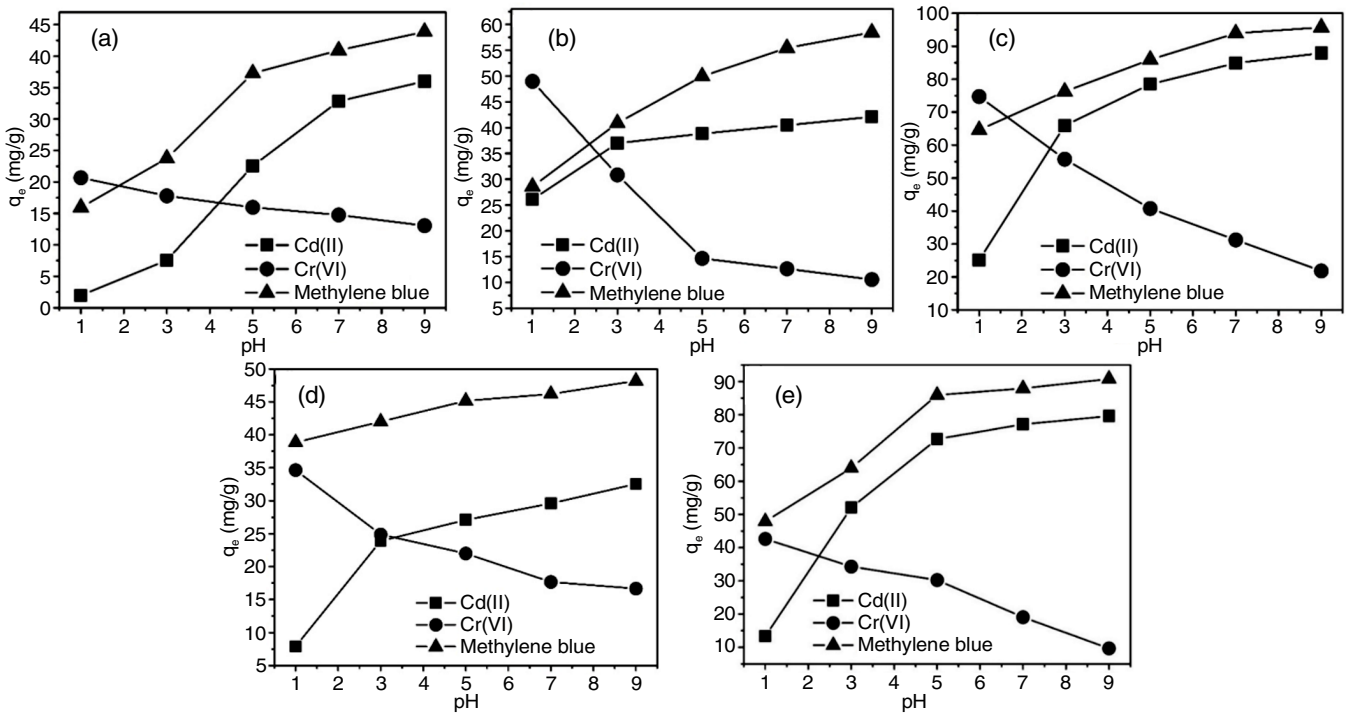

Fig. 3. Effect of pH on (a) PNS, (b) ANS, (c) CANS, (d) DNS and (e) CDNS

in weak electrostatic interactions because at acidic pH conditions the functional groups on the adsorbents surface are protonated and acquired positive charge [15,56]. Therefore, few active sites were available to react with Cd(II) ions and methylene blue [55]. However, as the pH increases the surface of the adsorbents gradually became deprotonated and acquired negative charge. Hence, there was higher uptake. This was also observed by Thabede *et al.* [57]. The maximum adsorption capacities for Cd(II) were 87.9, 79.6, 42.1, 36.0 and 32.6 mg/g onto CANS, CDNS, ANS, PNS and DNS at pH 9, respectively. On the other hand, methylene blue adsorption capacities were 95.7, 90.8, 58.4, 48.2 and 43.9 mg/g onto CANS, CDNS, ANS, DNS and PNS at pH 9, respectively. The results implied that percentage removal of Cd(II) and methylene blue by *Nigella sativa* seeds was lower in acidic medium which could due to the presence of positively charged hydrogen ions which competed and interfered with Cd(II) and methylene blue for the available adsorption sites [58]. It was observed that PNS, ANS, CANS, DNS and CDNS removed methylene blue more than Cr(VI) and Cd(II) ions.

Effect of contact time and kinetic parameters determination: The equilibration time and kinetics of PNS, ANS, CANS, DNS and CDNS sorption was determined in batch method by studying contact time. The adsorption rate of Cr(VI), Cd(II) and methylene blue onto PNS, ANS, CANS, DNS and CDNS *versus* time are shown in Fig. 4a-e. The trend of Cr(VI) onto all adsorbents in Fig. 4a-e showed that the adsorption rate was fast and happened in the first 10-15 min and thereafter, it became stable and reached equilibrium. The removal rate onto PNS, ANS, CANS, DNS and CDNS for Cd(II) was also quick in the beginning of the adsorption process within the first 20 min thereafter, the process slowed down and reached equilibrium. Methylene blue adsorption rate for PNS, ANS, CANS and DNS in Fig. 4a-d was observed between 15 and 20 min. On the other hand, the removal rate of methylene blue onto CDNS took place in the beginning of the process within 1 min and thereafter, no significant changes were observed. The adsorption of methylene blue was faster than Cr(VI) and Cd(II). The fast adsorption rate in the beginning of the process was due to abundant binding sites and availability of pores on adsorbents surfaces however, as time lapsed free binding sites and pores were consumed [33]. Thereafter, the rate slowed down because the binding sites and pores were exhausted and the adsorption was then controlled only by the rate at which Cr(VI), Cd(II) or methylene blue molecules are transported from the external to the internal sites of the adsorbents. This means that at initial stages, active sites were rapidly occupied by Cr(VI), Cd(II) and methylene blue molecules through chemical interaction and as time elapsed there were no more vacant sites on the adsorbents surfaces, so no multilayer was formed hence equilibrium was attained [59].

The chemical and physical features of adsorbents and adsorbates influence the rate of adsorption [60]. Hence, the results of Cr(VI), Cd(II) and methylene blue adsorption from aqueous solution onto PNS, ANS, CANS, DNS and CDNS surfaces were fitted into kinetic models. Pseudo-first order, pseudo-second order and intra-particle diffusion non-linear equations as indicated in eqns. 3-5, respectively were used to estimate the kinetic models. These equations were subjected to KyPlot software.

$$q_e = q_t\left(1 - e^{-k_1 t}\right) \quad (3)$$

$$q_e = \frac{1 + k_2 q_e t}{k_2 q_e^2 t} \quad (4)$$

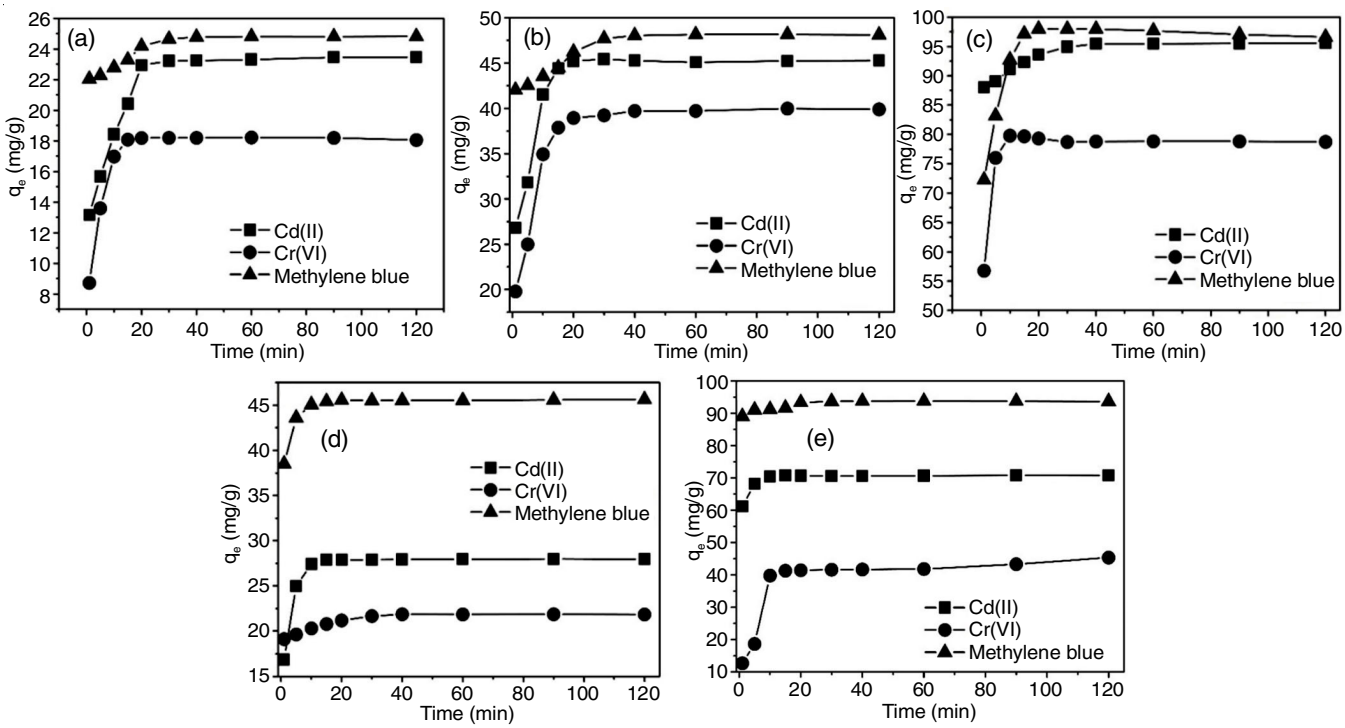

Fig. 4. Effect of time on (a) PNS, (b) ANS, (c) CANS, (d) DNS and (e) CDNS

$$q_t = k_i(t^{1/2}) + C \quad (5)$$

where q_e and q_t are the amount of adsorbate removed (mg/g) at equilibrium and time interval (t), respectively, (K_1) measured in min^{-1}; k_2 (g mg^{-1} min^{-1}) and K_i (g g^{-1} $min^{1/2}$) are the rate constants of the pseudo-first order in (1/min), pseudo-second order (g/mg/min) and intra-particle diffusion (g/g/$min^{-1/2}$), respectively and C (mg/g) is the adsorbate amount on the surface of the adsorbents. The pseudo-first order kinetic model assumes that the sorption rate depends on the number of the unoccupied sites in solution whilst the pseudo-second order kinetic model assumes that the sites on the adsorbent surface and adsorbate ions both determine the rate in the solution [60]. The nature of the adsorption process was also calculated using intra-particle diffusion kinetic model, which determines whether adsorption takes place on the surface (ESA) or pores (EPA). The calculation of ESA and EPA is based on the assumption that concentration (C) is equal to the obtained experimental (q_e) value, which means that the adsorption was due to surface (ESA) adsorption then ESA is equal to 100%. However, the remaining lower C value suggests that the adsorption was due to pore adsorption (EPA) [33].

Table-1 shows the kinetic models and the calculated parameters of all adsorbents. The kinetic models were used to predict the adsorption mechanism. The kinetic study of Cr(VI), Cd(II) and methylene blue onto PNS had a correlation value closest to 1 at 0.998, 0.993 and 0.998 for pseudo-first order and the calculated adsorption capacities of 19.98, 20.98 and 21.31 mg/g, respectively. The pseudo-first order results showed that they best fitted onto PNS than pseudo-second order. The calculated adsorption capacity for Cr(VI), Cd(II) and methylene blue onto ANS were 30.63, 40.76 and 46.93 mg/g and was close to the experimental data with r^2 values of 0.996, 0.997 and 0.996 which fitted pseudo-second order, respectively. Similarly, the calculated adsorption capacity of 81.44, 98.33 and 100.45 mg/g for Cr(VI), Cd(II) and methylene blue onto CANS best fitted pseudo-second order with r^2 values of 0.999, 0.998 and 0.994, respectively. The data for DNS and CDNS fitted pseudo-second order for Cr(VI), Cd(II) and methylene blue with r^2 values of 0.997, 0.995 and 0.995 onto DNS, whilst 0.998, 0.998 and 0.997 was observed onto CDNS. The calculated adsorption capacities of DNS were 22.99, 28.96 and 42.76 mg/g for Cr(VI), Cd(II) and methylene blue, respectively which was close to the experimental data. On the other hand, the experimental adsorption capacities of Cr(VI), Cd(II) and methylene blue onto CDNS were close to the calculated adsorption data which was 49.55, 75.06 and 95.52 mg/g, respectively. Intraparticle diffusion results indicated pore adsorption (EPA) for Cr(VI) and Cd(II) ions onto PNS were 52.23 and 53.70%, respectively whilst, the removal methylene blue was controlled by surface adsorption (ESA) with 85.78%. Intraparticle diffusion data showed that the removal of Cr(VI) was controlled by EPA with 55.54% onto ANS. On the other hand, Cd(II) and methylene blue adsorption onto ANS was due to ESA with 55.13 and 84.81%, respectively. The removal of Cr(VI), Cd(II) and methylene blue onto CANS was dominated by ESA with 70.11, 90.96, 72.90%, respectively. Similarly, Cr(VI), Cd(II) and methylene blue onto DNS was controlled by ESA with percentages of 72.38, 57.48 and 73.01%, respectively. The removals of Cr(VI) onto CDNS was controlled EPA with 77.35% whilst Cd(II) and methylene blue removal was due to ESP with 79.14 and 90.20%, respectively. The low (K_2) values suggested that the adsorption rate decreased with the increase of the phase contact time and the adsorption rate were proportional to the number of unoccupied sites [61].

Effect of concentration and equilibrium isotherms determination: The effect of initial concentration of Cr(VI), Cd(II) and methylene blue initial concentration onto PNS, ANS, CANS, DNS and CDNS was studied from 20, 40, 60, 80 and 100 mg/L are represented in Figs. 5a-e. The sorption capacity of Cd(II) and methylene blue onto PNS (Fig. 5a) increased with increasing initial concentration whilst the sorption of Cr(VI) showed a decreased between 80 to 100 mg/L. The maximum sorption capacities was found to be 17.77, 23.77 and 24.40 mg/g for Cr(VI), Cd(II) ions and methylene blue, respectively. The adsorption onto ANS and CANS (Fig. 5b-c) showed a similar pattern. The sorption of Cr(VI), Cd(II) and methylene blue had maximum adsorption capacities of 40.02, 48.41 and 49.02 mg/g onto ANS, respectively. Whereas the maximum sorption onto CANS were 77.81, 95.15 and 99.82 m/g for Cr(VI), Cd(II) and methylene blue, respectively. The increased in initial concentration was due to higher concentration gradient, which acted as a driving force to overcome resistances to mass transfer of ions between the aqueous phase and the solid phase [62]. In Fig. 5d-e, it was observed that as the initial concentration of Cr(VI) increased from 20 to 80 mg/L so did the adsorption

TABLE-1
KINETIC MODELS AND THEIR PARAMETERS ONTO PNS, ANS, CANS, DNS AND CDNS

Isotherms	PNS			ANS			CANS			DNS			CDNS		
	Cr(VI)	Cd(II)	MB	Cr(VI)	Cd(II)	MB	Cr(VI)	Cd(II)	MB	Cr(VI)	Cd(II)	MB	Cr(VI)	Cd(II)	MB
PFO q_e (mg g^{-1})	19.98	20.98	21.31	12.51	16.76	15.62	17.45	16.96	18.71	37.85	12.96	30.76	25.87	41.54	65.54
K_1 (min^{-1})	0.17	0.17	0.18	0.10	0.14	0.13	0.13	0.14	0.16	0.32	0.11	0.26	0.22	0.34	0.55
r^2	0.9982	0.993	0.998	0.8663	0.894	0.898	0.7815	0.888	0.789	0.799	0.869	0.896	0.755	0.968	0.896
PSO q_e (mg g^{-1})	11.27	11.98	10.89	30.63	40.76	46.93	81.44	98.33	100.45	22.85	28.96	42.76	49.55	75.06	95.52
K_2 ($mg^{(1-n)}$ L^n g^{-1})	0.094	0.099	0.091	0.26	0.34	0.39	0.68	0.82	0.84	0.19	0.24	0.36	0.41	0.63	0.80
r^2	0.859	0.907	0.98	0.996	0.997	0.996	0.999	0.998	0.994	0.997	0.995	0.995	0.998	0.998	0.997
IPD C (mg g^{-1})	8.70	10.82	21.29	17.77	25.50	20.85	55.96	86.98	71.44	15.83	16.09	33.32	11.18	56.04	84.56
K_i (g g^{-1} $min^{0.5}$)	0.073	0.090	0.18	0.15	0.21	0.17	0.47	0.72	0.60	0.13	0.13	0.28	0.093	0.47	0.70
r^2	0.86	0.88	0.92	0.72	0.96	0.89	0.97	0.89	0.91	0.86	0.90	0.95	0.89	0.79	0.98
EPA[a]%	52.23	53.70	14.22	55.54	44.86	15.19	29.89	9.04	27.10	27.62	42.52	26.99	77.35	20.86	9.80
ESA[a]%	47.77	46.30	85.78	44.65	55.14	84.81	70.11	90.96	72.90	72.38	57.48	73.01	24.65	79.14	90.20
Exp. (mg g^{-1})	18.22	23.46	24.82	39.38	45.44	48.17	79.81	95.62	97.99	21.87	27.99	45.64	45.36	70.81	93.75

MB = Methylene blue

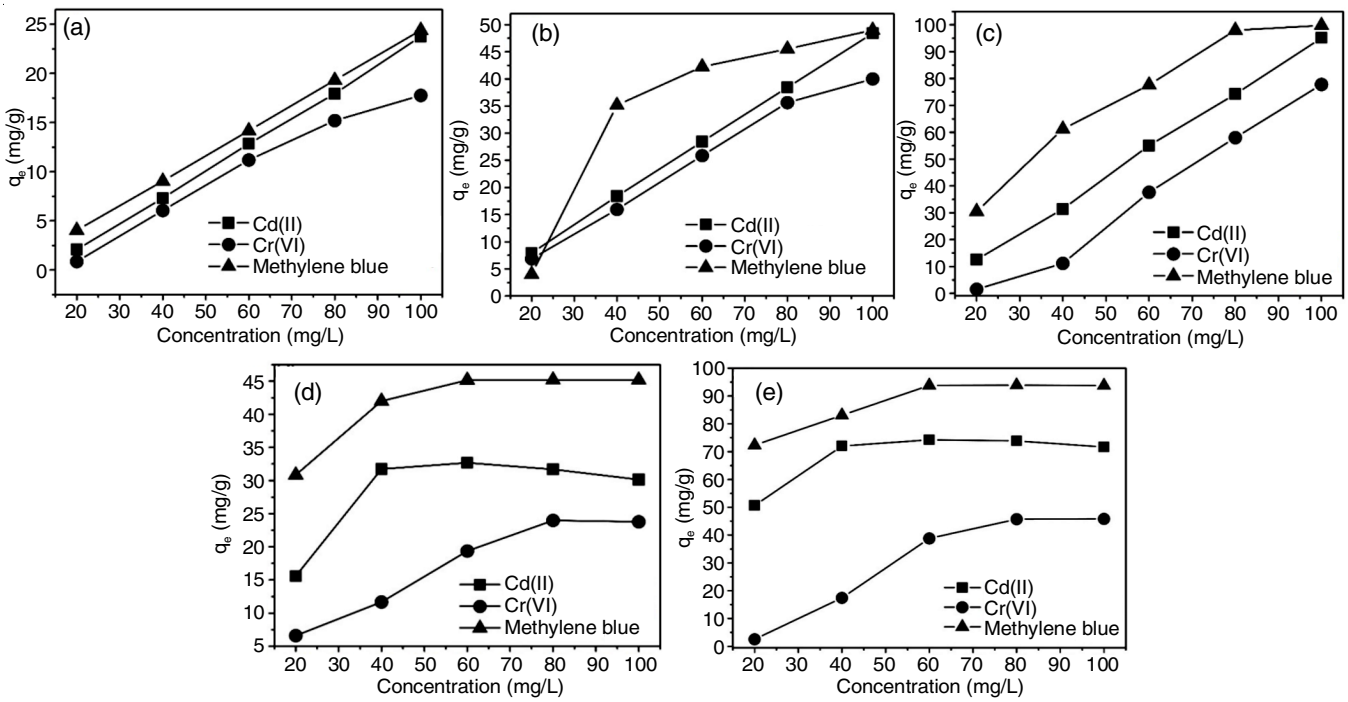

Fig. 5. Effects of concentration of Cd(II), Cr(VI) and methylene blue on (a) PNS, (b) ANS, (c) CANS, (d) DNS and (e) CDNS

capacity however a further increase of initial concentration between 80 and 100 mg/L gradually reduced to reach equilibrium. The adsorption of Cd(II) in Fig. 5d-e shows that the adsorption capacity increased between 20 and 40 mg/L thereafter, equilibrium was attained with a slight decrease. A similar observation was obtained for the removal of methylene blue in Fig. 5d-e where there was an increase in the initial concentration between 20 and 60 mg/L a further increase attained equilibrium. A decrease might be due to that the adsorbents had a certain number of active sites and at higher concentrations the active sites become saturated [63,64].

The non-linear adsorption isotherm models (Langmuir and Freundlich) were used to estimate the equilibrium data by using eqns. 6 and 7, respectively. Langmuir model proposes that the adsorption take place through chemisorption using monolayer adsorption of the sorbate on the adsorbent and is homogeneous in nature [65,66]. The model further calculates a saturation value of sorbent, as it suggests that the adsorbent has definite number of binding sites and each site is responsible for binding only one metal ion with almost zero interaction amongst the adsorbed ions [67]. On the contrary, the Freundlich model indicates multilayer sorption and is heterogeneous in nature [68].

$$q_e = \frac{Q_o b C_e}{1 + b C_e} \quad (6)$$

$$q_e = k_f C_e^{1/n} \quad (7)$$

Table-2 shows the adsorption models for Freundlich and Langmuir results for PNS, ANS, CANS, DNS and CDNS calculated at 298 K. The data showed coefficients for Cr(VI), Cd(II) and methylene blue with 0.9971, 0.993 and 0.998, respectively onto PNS which best fitted Freundlich model. Similarly, correlation coefficient onto ANS also fitted Freundlich model with r^2 of 0.996, 0.995 and 0.994 for Cr(VI), Cd(II) and methylene blue, respectively. This suggested that Cr(VI), Cd(II) and methylene blue onto PNS and ANS surface formed multilayer and was heterogeneous in nature [51]. The SEM images of PNS and ANS in Fig. 1b showed that the surfaces had rough structure development which was not homogenous. A similar observation was discovered by Chaudhry *et al.* [69]. The values (r^2) for CANS showed that they also fitted

TABLE-2
ADSORPTION ISOTHERM MODELS ONTO PNS, ANS, CANS, DNS AND CDNS

Isotherms	PNS			ANS			CANS			DNS			CDNS		
	Cr(VI)	Cd(II)	MB	Cr(VI)	Cd(II)	MB	Cr(VI)	Cd(II)	MB	Cr(VI)	Cd(II)	MB	Cr(VI)	Cd(II)	MB
Langmuir isotherm															
Q_o (mg g^{-1})	25.64	38.54	18.79	24.52	10.65	25.54	47.75	67.18	34.89	14.57	18.86	29.86	12.87	69.06	86.61
B (L mg^{-1})	0.21	0.32	0.16	0.20	0.089	0.21	0.39	0.56	0.29	0.12	0.16	0.25	0.11	0.56	0.72
r^2	0.883	0.874	0.819	0.864	0.913	0.886	0.895	0.969	0.955	0.906	0.896	0.881	0.855	0.886	0.896
Freundlich isotherm															
1/n (mg g^{-1})	19.27	21.74	27.51	43.63	43.12	42.63	90.35	72.06	94.55	23.31	31.06	48.06	41.85	73.26	97.72
k_f ($mg^{(1-n)}$ L^n g^{-1})	0.16	0.18	0.23	0.36	0.36	0.36	0.75	0.60	0.79	0.19	0.26	0.40	0.35	0.61	0.81
r^2	0.997	0.993	0.998	0.996	0.995	0.994	0.993	0.994	0.996	0.995	0.996	0.991	0.997	0.992	0.995
Exp. (mgg^{-1})	17.77	23.77	24.40	40.02	48.41	49.02	95.15	77.82	99.82	23.99	32.69	45.19	45.81	74.26	93.90

Freundlich model than Langmuir model and the correlation values for Cr(VI), Cd(II) and methylene blue were 0.993, 0.994 and 0.996, respectively. The equilibrium data indicated that the sorption results for Cr(VI), Cd(II) and methylene blue onto DNS fitted Freundlich model with high r^2 of 0.995, 0.996 and 0.991. Similarly, the regression values (r^2) for Cr(VI), Cd(II) and methylene blue fitted Freundlich model onto CDNS.

Temperature effect and thermodynamic parameters determination: The sorption of Cr(VI), Cd(II) and methylene blue onto PNS, ANS, CANS, DNS and CDNS are shown in Fig. 6a-e. The patterns in Fig. 6a-e shows that the removal of Cd(II) and methylene blue increased as the temperature increased from 298 to 303 K thereafter equilibrium was reached on all adsorbents. The maximum sorption capacities of Cd(II) onto PNS, ANS, CANS, DNS and CDNS were 23.46, 48.11, 96.89, 31.37 and 73.91 mg/g, respectively whilst methylene blue capacities were 24.44, 48.60, 97.97, 45.92 and 92.60 mg/g, respectively. This increase in temperature was important because it showed that high temperature was required so that the ions in the solution had enough kinetic energy to overcome obstructing the sorption process [70]. Fig. 6a-e showed that the sorption of Cr(VI) onto PNS, ANS, CANS, DNS and CDNS increased as temperature increased from 298 to 353 K. This showed the endothermic nature of the sorption processes [15], with maximum sorption capacities of 19.84, 42.48, 87.44, 29.99 and 65.38 mg/g, respectively onto PNS, ANS, CANS, DNS and CDNS. The gradually increased adsorption at higher temperatures indicated that adsorbate-adsorbent interaction was feasible at higher temperatures, suggesting that higher temperatures were more favourable to the adsorption process [59].

Thermodynamic parameters are significant tools to check the feasibility and spontaneity of the adsorption process [69]. Thermodynamic entropy change (ΔS°) and enthalpy change (ΔH°) and Gibbs free energy change (ΔG°) were assessed using eqns. 8 and 9. ΔH° and ΔS° were attained from the slope and intercept of the van't Hoff plot of ln K against 1/T. And K_c is the equilibrium constant of thermodynamic function which was calculated by eqn. 10, where q_e is the amount of Cr(VI), Cd(II) and methylene blue adsorbed per unit mass of samples (mg/g) onto PNS, ANS, CANS, DNS and CDNS.

$$\ln K_c = -\frac{\Delta H^\circ}{RT} - \frac{\Delta S^\circ}{R} \tag{8}$$

$$\Delta G^\circ = -RT \ln K_c \tag{9}$$

$$K_c = \frac{q_e}{C_e} \tag{10}$$

Thermodynamic parameters (ΔS°, ΔH° and ΔG°) for Cr(VI), Cd(II) and methylene blue are shown in Table-3 for PNS, ANS, CANS, DNS and CDNS calculated at 298, 303, 313, 333 and 353 K. The sorption processes of Cr(VI), Cd(II) and methylene blue indicated positive values for (ΔS° and ΔH°) on all adsorbents. The positive values for (ΔS°) suggested the increased randomness of the ions in the solution as the adsorption processes approached equilibrium [71] meanwhile the positive (ΔH°) indicated that the reaction was endothermic. An endothermic reaction increased the removal uptake of Cr(VI), Cd(II) and methylene blue as temperature of the system was increased, this was in agreement with temperature effect results [15]. The calculated (ΔG°) values were negative for PNS, ANS, CANS, DNS and CDNS in all the investigated temperatures and became more negative with an increase in temperature. The negative values indicated that the removal of Cr(VI), Cd(II) and methylene blue on all the adsorbents were

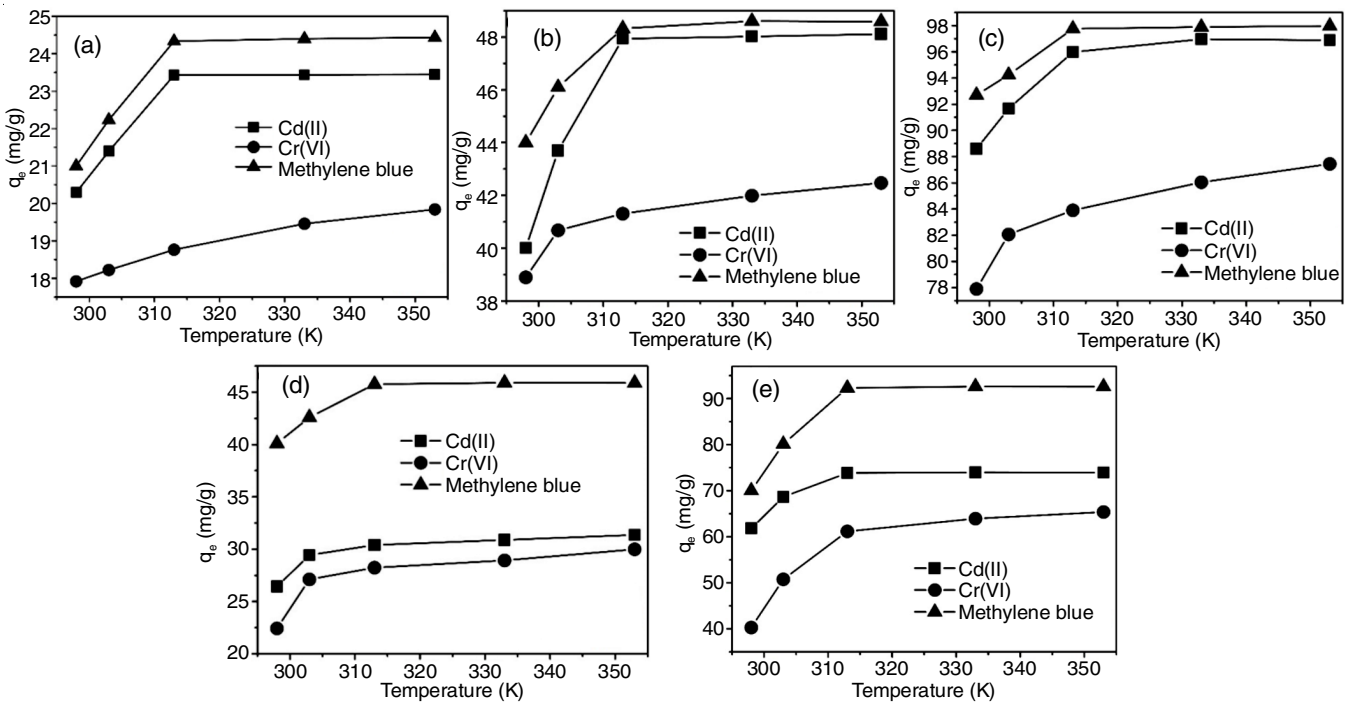

Fig. 6. Effects of temperature on (a) PNS, (b) ANS, (c) CANS, (d) DNS and (e) CDNS

TABLE-3
THERMODYNAMIC PARAMETERS PNS, ANS, CANS, DNS AND CDNS

Parameter	PNS			ANS			CANS			DNS			CDNS		
	Cr(VI)	Cd(II)	MB	Cr(VI)	Cd(II)	MB	Cr(VI)	Cd(II)	MB	Cr(VI)	Cd(II)	MB	Cr(VI)	Cd(II)	MB
ΔH^o (KJ mol^{-1})	4×10^{-4}	4×10^{-3}	8×10^{-4}	1×10^{-4}	1×10^{-3}	9×10^{-4}	9×10^{-4}	8×10^{-4}	5×10^{-4}	7×10^{-4}	1×10^{-3}	2×10^{-3}	4×10^{-4}	2×10^{-3}	5×10^{-3}
ΔS^o (KJ mol^{-1} K^{-1})	2×10^{-4}	8×10^{-3}	5×10^{-3}	4×10^{-4}	6×10^{-3}	5×10^{-4}	4×10^{-3}	6×10^{-3}	4×10^{-4}	3×10^{-3}	2×10^{-3}	7×10^{-3}	3×10^{-4}	5×10^{-3}	1×10^{-3}
ΔG^o (KJ mol^{-1})															
288 K	-7.70	-3.04	-4.44	-1.91	-6.11	-5.63	-3.21	-7.62	-7.69	-2.23	-9.43	-3.78	-9.49	-2.19	-6.06
298 K	-7.65	-3.26	-5.20	-1.75	-6.37	-5.89	-3.83	-8.48	-8.96	-1.32	-8.41	-4.15	-8.82	-2.34	-6.19
308 K	-7.40	-3.42	-5.78	-1.32	-6.93	-6.13	-4.29	-9.03	-9.03	-1.12	-6.60	-4.40	-7.49	-2.70	-6.47
318 K	-7.20	-2.82	-6.42	-1.28	-7.33	-6.65	-4.81	-9.59	-9.25	-1.06	-5.89	-4.78	-6.69	-2.89	-7.00
328 K	-7.11	-3.99	-7.06	-1.21	-7.23	-7.56	-5.19	-9.81	-9.51	-1.01	-5.05	-5.05	-4.70	-3.06	-7.42

spontaneous and feasible [72]. Physical adsorption of Gibb's free energy change (ΔG^o) ranges between -20 and 0 kJ/mol whilst the chemical adsorption is between -80 to -400 kJ/mol [73]. Therefore, the data in Table-3 showed that the adsorption process was predominated by physical adsorption process. This indicated that higher adsorption occurred at higher temperatures and that at higher temperature and ions were readily desolvated and their adsorption becomes more favourable [74].

Comparative sorption studies of Cr(VI), Cd(II) and methylene blue dye: A comparative study of sorption capacities of different adsorbents are presented in Table-4. The defatted and carbonized *Nigella sativa* adsorbents of ANS, CANS, DNS and CDNS adsorption capacities for Cr(VI), Cd(II) and methylene blue were compared with other adsorbents from literature. The comparison studies showed that ANS, CANS, DNS and CDNS had higher adsorption capacities than some of the reported adsorbents. Therefore, defatted *Nigella sativa* L. seeds can be used as low cost adsorbents for the removal of Cr(VI), Cd(II) and methylene blue in aqueous solution.

Reusability studies: The reusability of adsorbents is an important factor for its practical application. In order to make the adsorption process inexpensive, it is vital that the adsorbent display significant properties such as the ability to regenerate, high adsorption capacity and be able to be reusable in the adsorption process [51]. The reusability of PNS, ANS, CANS, DNS and CDNS were investigated using 0.01 M HCl as an eluting agent and distilled water. The adsorption/desorption results of the adsorbents for Cr(VI), Cd(II) and methylene blue are shown in Fig. 7a-e. The data showed that originally PNS, ANS, CANS, DNS and CDNS displayed high removal uptake. After four cycles of adsorption-desorption the removal percentages decreased for all adsorbents. This might be due to inability of the adsorbents to desorb metal ions and dye from the adsorbents surface and cavities during the regeneration processes [95] and the mass loss of the adsorbents during desorption [62] hence the lower uptake. These findings indicated that PNS, ANS, CANS, DNS and CDNS adsorbents may be reusable in aqueous solution for treatment.

Conclusion

The effectiveness of the defatted and carbonized *Nigella sativa* L. seeds was studied in batch experiments for the removal of Cr(VI), Cd(II) and methylene blue in aqueous solution. *Nigella sativa* L. seeds were defatted using different solvents such as acetone and DMF thereafter carbonized at 600 ºC. The defatted and the carbon defatted seeds were compared with the pristine *Nigella sativa* L. (PNS) seeds. A series of adsorption tests were conducted using different parameters namely; contact time, initial concentration, temperature and pH. The adsorption of Cr(VI), Cd(II) and methylene blue was influenced by the solution pH. The high Cr(VI) removal was observed at pH 1 on all adsorbents whilst the maximum adsorption capacities for Cd(II) and methylene blue were at pH 9. SEM images showed different surface morphological properties with distinct cavities and pore structures resulting from the defatted the *Nigella sativa* seeds. The FTIR spectra of PNS, ANS, DNS and CDNS showed shifts in transmission frequencies which suggested that there was interaction of adsorbents with the adsorbates. The adsorption of Cr(VI), Cd(II) and methylene blue was fast ranging from 1 and 20 min thereafter, the rate slowed

TABLE-4
LITERATURE REPORTS OF ACTIVATED CARBON MATERIALS FOR THE REMOVAL OF Cr(VI) IONS, Cd(II) IONS AND METHYLENE BLUE

Cr(II) ions			Cd(II) ions			Methylene blue		
Adsorbent	Maximum capacity (mg/g)	Ref.	Adsorbent	Maximum capacity (mg/g)	Ref.	Adsorbent	Maximum capacity (mg/g)	Ref.
Peanut shell	106.4	[27]	*Glebionis coronaria L.*	106.9	[81]	*Magnolia grandiflora* L.	101.3	[88]
Defatted *Nigella sativa* L.	87.44	This study	Defatted AC *Nigella sativa* L.	96.89	This study	Defatted *Nigella sativa* L.	99.82	This study
Carbon microsphere	65.5	[75]	Rice straw	74.6	[82]	Licorice root waste	82.9	[89]
Peganum harmala seed	53.5	[76]	*Trapa natans* husks	50.2	[83]	Reed	77.4	[90]
Pinewood sawdust	42.7	[77]	*Phragmites australis*	40.6	[84]	Coconut bunch waste	70.9	[91]
Macadamia	40.9	[78]	Buffalo weed	11.6	[85]	*Ficus carica* bast	49.9	[92]
Bamboo bark	18.9	[79]	Chicken feather	7.8	[86]	Activated lignin-chitosan	36.2	[93]
Carbon nanotubes	14.3	[80]	Oxidized granular AC	5.7	[87]	Feldspar clay	19.9	[94]

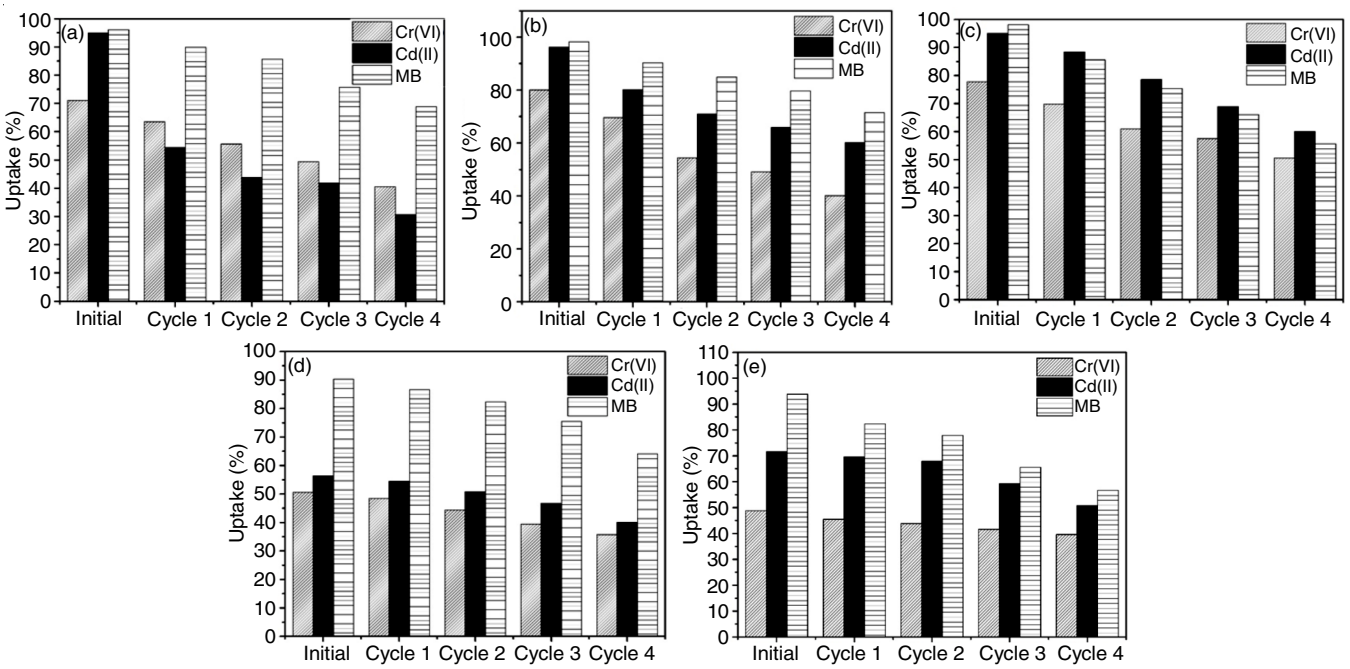

Fig. 7. Regeneration studies on (a) PNS, (b) ANS, (c) CANS, (d) DNS and (e) CDNS

down due to exhaustion of the pores and binding sites. The kinetic models predicted the adsorption mechanism of Cr(VI), Cd(II) and methylene blue onto PNS as pseudo-first order, which suggested that the rate of adsorption depended on the unoccupied sites. On the other hand, the adsorption mechanism onto ANS, CANS, DNS and CDNS showed a good fit for pseudo second order, which indicated that the sites on the adsorbents surface and the adsorbate ions and the dye played a key role in the adsorption rate. The effect of concentration showed that the adsorption capacity increased with increasing initial concentration. The high correlation coefficient r^2 showed that PNS and ANS best fitted Freundlich model, which proposed multilayer formation of adsorbate and heterogeneous in nature. However the adsorption of Cr(VI), Cd(II) and methylene blue onto CANS, DNS and CDNS fitted to Langmuir isotherm which assumed that the adsorption took place through monolayer and was a homogenous process. The adsorption capacities of all adsorbents increased with temperatures indicated that the process was feasible at higher temperatures and also the high temperatures were favourable for the adsorption process. The values of ΔS° and ΔH° were positive for the sorption of Cr(VI), Cd(II) and methylene blue on all adsorbents suggested that the reaction was endothermic. The ΔG° values were negative for PNS, ANS, CANS, DNS and CDNS for all temperatures and more negative with an increase in temperature. This indicated that the removal of Cr(VI), Cd(II) and methylene blue on all the adsorbents were spontaneous and feasible. The results showed that CANS had highest adsorption capacity of 99.82 mg/g for methylene blue, 96.89 m/g for Cd(II) and 87.44 mg/g for Cr(VI) compared to CDNS, ANS, DNS and PNS. The capacity trend was CANS > CDNS > ANS > DNS > PNS. The reusability results showed the black cumin seeds adsorbents can be recycled for the adsorption of Cr(VI), Cd(II) and methylene blue from aqueous solution. This presents potential advantages such easy generation of the adsorbents and their ability to be reused more than three times.

ACKNOWLEDGEMENTS

The authors acknowledge to The National Research Fund (NRF) for sponsoring this research and the Vaal University of Technology is greatly appreciated.

CONFLICT OF INTEREST

The authors declare that there is no conflict of interests regarding the publication of this article.

REFERENCES

1. J. Serrano-Gomez, H. Lopez-Gonzalez, M.T. Olguin and S. Bulbulian, *J. Environ. Manage.*, **156**, 121 (2015); https://doi.org/10.1016/j.jenvman.2015.03.013
2. Z. Heidarinejad, M.H. Dehghani, M. Heidari, G. Javedan, I. Ali and M. Sillanpää, *Environ. Chem. Lett.*, **18**, 393 (2020); https://doi.org/10.1007/s10311-019-00955-0
3. R. Goswami, J. Shim, S. Deka, D. Kumari, R. Kataki and M. Kumar, *Ecol. Eng.*, **97**, 444 (2016); https://doi.org/10.1016/j.ecoleng.2016.10.007
4. S.I. Siddiqui and S.A. Chaudhry, *Curr. Environ. Eng.*, **4**, 81 (2017); https://doi.org/10.2174/2212717804666161214143715
5. A. Pugazhendhi, G.M. Boovaragamoorthy, K. Ranganathan, M. Naushad and T. Kaliannan, *J. Clean. Prod.*, **174**, 1234 (2018); https://doi.org/10.1016/j.jclepro.2017.11.061
6. S.I. Siddiqui, S.A. Chaudhry, S.U. Islam and S.U. Islam, Plant-based Natural Products: Derivatives and Applications. John Wiley & Sons, Inc., p. 193 (2017).
7. M. Priyanka and M.P. Saravanakumar, *J. Clean. Prod.*, **197**, 511 (2018); https://doi.org/10.1016/j.jclepro.2018.06.197
8. C. Santhosh, P. Kollu, S. Doshi, M. Sharma, M. Vanchinathan, D. Bahadur, P. Saravanan, B.-S. Kim and A.N. Grace, *RSC Adv.*, **4**, 28300 (2014); https://doi.org/10.1039/C4RA02913E
9. H. Gali-Muhtasib, N. El-Najjar and R. Schneider-Stock, *Adv. Phytomed.*, **2**, 133 (2006); https://doi.org/10.1016/S1572-557X(05)02008-8

10. M.A.O. Adam and M.A.S. Shakak, *GCNU J.*, 236 (2019).
11. M. Ardiana, B.S. Pikir, A. Santoso, H.O. Hermawan and M.J. Al-Farabi, *Scientific World J.*, **2020**, 2390706 (2020); https://doi.org/10.1155/2020/2390706
12. U. Erdogan, M. Yilmazer and S. Erbas, *Bilge Int. J. Sci. Technol.*, **4**, 27 (2020); https://doi.org/10.30516/bilgesci.688845
13. R. Ahmad and S. Haseeba, *Desalin. Water Treat.*, **56**, 2512 (2014); https://doi.org/10.1080/19443994.2014.968627
14. S. Begum and A. Mannan, *J. Drug Deliv. Ther.*, **10**, 213 (2020); https://doi.org/10.22270/jddt.v10i2.3913
15. P.M. Thabede, N.D. Shooto and E.B. Naidoo, *S. Afr. J. Chem. Eng.*, **33**, 39 (2020); https://doi.org/10.1016/j.sajce.2020.04.002
16. Z.N. Garba, I. Bello, A. Galadima and A.Y. Lawal, *Karbala Int. J. Modern Sci.*, **2**, 20 (2016); https://doi.org/10.1016/j.kijoms.2015.12.002
17. M.A. Al-Anber, Z.A. Al-Anber, I. Al-Momani, F. Al-Momani and Q. Abu-Salem, *Desalination Water Treat.*, **52**, 293 (2014); https://doi.org/10.1080/19443994.2013.784878
18. T.S. Chandra, S.N. Mudliar, S. Vidyashankar, S. Mukherji, R. Sarada, K. Krishnamurthi and V.S. Chauhan, *Bioresour. Technol.*, **184**, 395 (2015); https://doi.org/10.1016/j.biortech.2014.10.018
19. Y. Xie, S. Holmgren, D.M.K. Andrews and M.S. Wolfe, *Environ. Health Perspect.*, **125**, 81 (2017); https://doi.org/10.1289/EHP21
20. A. Al-Futaisi, A. Jamrah and R. Al-Hanai, *Desalin.*, **214**, 327 (2007); https://doi.org/10.1016/j.desal.2006.10.024
21. A.A. Narvekar, J.B. Fernandes and S.G. Tilve, *J. Environ. Chem. Eng.*, **6**, 1714 (2018); https://doi.org/10.1016/j.jece.2018.02.016
22. Z. Anfar, R. El Haouti, S. Lhanafi, M. Benafqir, Y. Azougarh and N. El Alem, *J. Environ. Chem. Eng.*, **5**, 5857 (2017); https://doi.org/10.1016/j.jece.2017.11.015
23. S. Cengiz and L. Cavas, *Bioresour. Technol.*, **99**, 2357 (2008); https://doi.org/10.1016/j.biortech.2007.05.011
24. M.M. Islam, M.N. Khan, A.K. Mallik and M.M. Rahman, *J. Hazard. Mater.*, **379**, 120792 (2019); https://doi.org/10.1016/j.jhazmat.2019.120792
25. K.L. Palanisamy, V. Devabharathi and N.M. Sundaram, *Int. J. Res. Appl. Nat. Soc. Sci.*, **1**, 15 (2013).
26. A. Alemu, B. Lemma, N. Gabbiye, M.T. Alula and M.T. Desta, *Heliyon*, **4**, e00682 (2018); https://doi.org/10.1016/j.heliyon.2018.e00682
27. M. Gueye, Y. Richardson, F.T. Kafack and J. Blin, *J. Environ. Chem. Eng.*, **2**, 273 (2014); https://doi.org/10.1016/j.jece.2013.12.014
28. N. Zhou, Y. Wang, D. Yao, S. Li, J. Tang, D. Shen, X. Zhu, L. Huang, M. Zhong and Z. Zhou, *J. Clean. Prod.*, **221**, 63 (2019); https://doi.org/10.1016/j.jclepro.2019.02.176
29. A. Aghababaei, M.C. Ncibi and M. Sillanpaa, *Bioresour. Technol.*, **239**, 28 (2017); https://doi.org/10.1016/j.biortech.2017.04.119
30. U.A. Gilbert, I.U. Emmanuel, A.A. Adebanjo and G.A. Olalere, *Biomass Bioenergy*, **35**, 2517 (2011); https://doi.org/10.1016/j.biombioe.2011.02.024
31. K.D. Kowanga, E. Gatebe, G.O. Mauti and E.M. Mauti, *J. Phytopharmacology*, **5**, 71 (2016).
32. J.T. da Fontoura, G.S. Rolim, B. Mella, M. Farenzena and M. Gutterres, *J. Environ. Chem. Eng.*, **5**, 5076 (2017); https://doi.org/10.1016/j.jece.2017.09.051
33. N.D. Shooto, C.S. Nkutha, N.R. Guilande and E.B. Naidoo, *S. Afr. J. Chem. Eng.*, **31**, 33 (2020); https://doi.org/10.1016/j.sajce.2019.12.001
34. D. Lu, Q. Cao, X. Li, X. Cao, F. Luo and W. Shao, *Hydrometallurgy*, **95**, 145 (2009); https://doi.org/10.1016/j.hydromet.2008.05.008
35. N.D. Shooto, P.M. Thabede, B. Bhila, H. Moloto and E.B. Naidoo, *J. Environ. Chem. Eng.*, **8**, 103557 (2020); https://doi.org/10.1016/j.jece.2019.103557
36. M. Asgher and H.N. Bhatti, *Ecol. Eng.*, **38**, 79 (2012); https://doi.org/10.1016/j.ecoleng.2011.10.004
37. R.N. Oliveira, M.C. Mancini, F.C.S.D. Oliveira, T.M. Passos, B.R.M.D. Quilty, M. Thire and G.B. McGuinness, *Matéria (Rio de Janeiro)*, **21**, 767 (2016); https://doi.org/10.1590/S1517-707620160003.0072
38. M. Dahiru, Z.U. Zango and M.A. Haruna, *Am. J. Mater. Sci.*, **8**, 32 (2018).
39. Z. Heidarinejad, O. Rahmanian, M. Fazlzadeh and M. Heidari, *J. Mol. Liq.*, **264**, 591 (2018); https://doi.org/10.1016/j.molliq.2018.05.100
40. R. Nagarjuna, M.S.M. Saifullah and R. Ganesan, *RSC Adv.*, **8**, 11403 (2018); https://doi.org/10.1039/C8RA01688G
41. H. Zhang, J. Zhou, Y. Muhammad, R. Tang, K. Liu, Y. Zhu and Z. Tong, *Front. Mater.*, **6**, 5 (2019); https://doi.org/10.3389/fmats.2019.00005
42. M. Danish, T. Ahmad, R. Hashim, N. Said, M.N. Akhtar, J. Mohamad-Saleh and O. Sulaiman, *Surf. Interfaces*, **11**, 1 (2018); https://doi.org/10.1016/j.surfin.2018.02.001
43. N.D. Shooto, P.M. Thabede and E.B. Naidoo, *S. Afr. J. Chem. Eng.*, **30**, 15 (2019); https://doi.org/10.1016/j.sajce.2019.07.002
44. O.E. Abdel-Salam, M.A. Shoeib and H.A. Elkilany, *Egypt. J. Pet.*, **27**, 497 (2018); https://doi.org/10.1016/j.ejpe.2017.07.014
45. Y. Tang, L. Chen, X. Wei, Q. Yao and T. Li, *J. Hazard. Mater.*, **244-245**, 603 (2013); https://doi.org/10.1016/j.jhazmat.2012.10.047
46. A.S. Yusuff, *J. Arab Basic Appl.*, **26**, 89 (2019); https://doi.org/10.1080/25765299.2019.1567656
47. Z. Shen, J. Zhang, D. Hou, D.C.W. Tsang, Y.S. Ok and D.S. Alessi, *Environ. Int.*, **122**, 357 (2019); https://doi.org/10.1016/j.envint.2018.11.045
48. J. Bai, H. Yao, F. Fan, M. Lin, L. Zhang, H. Ding, F. Lei, X. Wu, X. Li, J. Guo and Z. Qin, *J. Environ. Radioact.*, **101**, 969 (2010); https://doi.org/10.1016/j.jenvrad.2010.07.003
49. E.I. Unuabonah, G.U. Adie, L.O. Onah and O.G. Adeyemi, *Chem. Eng. J.*, **155**, 567 (2009); https://doi.org/10.1016/j.cej.2009.07.012
50. S.A. Chaudhry, Z. Zaidi and S.I. Siddiqui, *J. Mol. Liq.*, **229**, 230 (2017); https://doi.org/10.1016/j.molliq.2016.12.048
51. A. Aichour, H. Zaghouane-Boudiaf, C.V. Iborra and M.S. Polo, *J. Mol. Liq.*, **256**, 533 (2018); https://doi.org/10.1016/j.molliq.2018.02.073
52. B.K. Nandi, A. Goswami and M.K. Purkait, *J. Hazard. Mater.*, **161**, 387 (2009); https://doi.org/10.1016/j.jhazmat.2008.03.110
53. Q. Liu, Q. Liu, B. Liu, T. Hu, W. Liu and J. Yao, *J. Hazard. Mater.*, **352**, 27 (2018); https://doi.org/10.1016/j.jhazmat.2018.02.040
54. Z. Jia, Y. Shu, R. Huang, J. Liu and L. Liu, *Chemosphere*, **199**, 232 (2018); https://doi.org/10.1016/j.chemosphere.2018.02.021
55. H. Huang, Y. Wang, Y. Zhang, Z. Niu and X. Li, *Open Chem.*, **18**, 97 (2020); https://doi.org/10.1515/chem-2020-0009
56. X. Li, S.F. Wang, Y.G. Liu, L.H. Jiang, B.A. Song, M.F. Li, G. Zeng, X. Tan, X. Cai and Y. Ding, *J. Chem. Eng. Data*, **62**, 407 (2017); https://doi.org/10.1021/acs.jced.6b00746
57. P.M. Thabede, N.D. Shooto, T. Xaba and E.B. Naidoo, *J. Environ. Chem. Eng.*, **8**, 104045 (2020); https://doi.org/10.1016/j.jece.2020.104045
58. T. Salman, F. Temel, N. Turan and Y. Ardali, *Glob. NEST J.*, **18**, 1 (2016).
59. A.S.K. Kumar and S-J. Jiang, *Mol. Liq.*, **237**, 387 (2017); https://doi.org/10.1016/j.molliq.2017.04.093
60. S.I. Siddiqui and S.A. Chaudhry, *J. Clean. Prod.*, **200**, 996 (2018); https://doi.org/10.1016/j.jclepro.2018.07.300
61. D. Kolodynska, J. Krukowska and P. Thomas, *Chem. Eng. J.*, **307**, 353 (2017); https://doi.org/10.1016/j.cej.2016.08.088

62. K.G. Akpomie, F.A. Dawodu and K.O. Adebowale, *Alexandria Eng. J.*, **54**, 757 (2015); https://doi.org/10.1016/j.aej.2015.03.025
63. J. Huang, M. Ye, Y. Qu, L. Chu, R. Chen, Q. He and D. Xu, *J. Colloid Interface Sci.*, **385**, 137 (2012); https://doi.org/10.1016/j.jcis.2012.06.054
64. F.A. Olabemiwo, B.S. Tawabini, F. Patel, T.A. Oyehan, M. Khaled and T. Laoui, *Bioinorg. Chem. Appl.*, **2017**, 7298351 (2017); https://doi.org/10.1155/2017/7298351
65. I. Aloma, M.A. Martin-Lara, I.L. Rodriguez, G. Blazquez and M. Calero, *J. Taiwan Inst. Chem. Eng.*, **43**, 275 (2012); https://doi.org/10.1016/j.jtice.2011.10.011
66. M. Basu, A.K. Guha and L. Ray, *Process Saf. Environ.*, **106**, 11 (2017); https://doi.org/10.1016/j.psep.2016.11.025
67. A. Shokrollahi, A. Alizadeh, Z. Malekhosseini and M. Ranjbar, *J. Chem. Eng. Data*, **56**, 3738 (2011); https://doi.org/10.1021/je200311y
68. A. Saeed, M. Iqbal and W.H. Holl, *J. Hazard. Mater.*, **168**, 1467 (2009); https://doi.org/10.1016/j.jhazmat.2009.03.062
69. S.A. Chaudhry, T.A. Khan and I. Ali, *Egypt. J. Basic Appl. Sci.*, **3**, 287 (2016); https://doi.org/10.1016/j.ejbas.2016.06.002
70. A. Aichour and H. Zaghouane-Boudiaf, *Microchem. J.*, **146**, 1255 (2019); https://doi.org/10.1016/j.microc.2019.02.040
71. L. Shifera, K. Siraj and A. Yifru, *Indian J. Chem. Technol.*, **24**, 145 (2016).
72. I.H. Ali, M.K. Al Mesfer, M.I. Khan, M. Danish and M.M. Alghamdi, *Processes*, **7**, 217 (2019); https://doi.org/10.3390/pr7040217
73. M.R. Awual, I.M.M. Rahman, T. Yaita, M.A. Khaleque and M. Ferdows, *Chem. Eng. J.*, **236**, 100 (2014); https://doi.org/10.1016/j.cej.2013.09.083
74. F.M. Winnik, *Langmuir*, **34**, 1 (2018); https://doi.org/10.1021/acs.langmuir.7b04375
75. R. Khosravi, G. Moussavi, M.T. Ghaneian, M.H. Ehrampoush, B. Barikbin, A.A. Ebrahimi and G. Sharifzadeh, *J. Mol. Liq.*, **256**, 163 (2018); https://doi.org/10.1016/j.molliq.2018.02.033
76. P. Yang, D. Guo, Z. Chen, B. Cui, B. Xiao, S. Liu and M. Hu, *J. Dispers. Sci. Technol.*, **38**, 1665 (2017); https://doi.org/10.1080/01932691.2016.1272058
77. M. Lesaoana, R.P.V. Mlaba, F.M. Mtunzi, M.J. Klink, P. Ejidike and V.E. Pakade, *S. Afr. J. Chem. Eng.*, **28**, 8 (2019); https://doi.org/10.1016/j.sajce.2019.01.001
78. Y.-J. Zhang, J.-L. Ou, Z.-K. Duan, Z.-J. Xing and Y. Wang, *Colloids Surf. A Physicochem. Eng. Asp.*, **481**, 108 (2015); https://doi.org/10.1016/j.colsurfa.2015.04.050
79. S.S. Bayazit and O. Kerkez, *Chem. Eng. Res. Des.*, **92**, 2725 (2014); https://doi.org/10.1016/j.cherd.2014.02.007
80. H. Tounsadi, A. Khalidi, M. Farnane, M. Abdennouri and N. Barka, *Process Saf. Environ. Prot.*, **102**, 710 (2016); https://doi.org/10.1016/j.psep.2016.05.017
81. Z. Zhang, X. Yue, W. Xu, H. Zhang and F. Li, *J. Hazard. Mater.*, **379**, 120783 (2019); https://doi.org/10.1016/j.jhazmat.2019.120783
82. W. Yin, C. Zhao, J. Xu, J. Zhang, Z. Guo and Y. Shao, *Colloids Surf. A Physicochem. Eng. Asp.*, **560**, 426 (2019); https://doi.org/10.1016/j.colsurfa.2018.10.031
83. Z. Guo, X. Zhang, Y. Kang and J. Zhang, *ACS Sustain. Chem. Eng.*, **5**, 4103 (2017); https://doi.org/10.1021/acssuschemeng.7b00061
84. K. Yakkala, M.-R. Yu, H. Roh, J.-K. Yang and Y.-Y. Chang, *Desalination Water Treat.*, **51**, 7732 (2013); https://doi.org/10.1080/19443994.2013.792546
85. H. Chen, W. Li, J. Wang, H. Xu, Y. Liu, Z. Zhang, Y. Li and Y. Zhang, *Bioresour. Technol.*, **292**, 121948 (2019); https://doi.org/10.1016/j.biortech.2019.121948
86. X. Huang, N.Y. Gao and Q.L. Zhang, *J. Environ. Sci.*, **19**, 1287 (2007); https://doi.org/10.1016/S1001-0742(07)60210-1
87. B. Ji, J. Wang, H. Song and W. Chen, *J. Environ. Chem. Eng.*, **7**, 103036 (2019); https://doi.org/10.1016/j.jece.2019.103036
88. M. Ghaedi, M.D. Ghazanfarkhani, S. Khodadoust, N. Sohrabi and M. Oftade, *J. Ind. Eng. Chem.*, **20**, 2548 (2014); https://doi.org/10.1016/j.jiec.2013.10.039
89. Y. Wang, Y. Zhang, S. Li, W. Zhong and W. Wei, *J. Mol. Liq.*, **268**, 658 (2018); https://doi.org/10.1016/j.molliq.2018.07.085
90. B.H. Hameed, D.K. Mahmoud and A.L. Ahmad, *J. Hazard. Mater.*, **158**, 65 (2008); https://doi.org/10.1016/j.jhazmat.2008.01.034
91. D. Pathania, S. Sharma and P. Singh, *Arab. J. Chem.*, **10**, S1445 (2017); https://doi.org/10.1016/j.arabjc.2013.04.021
92. A.B. Albadarin, M.N. Collins, M. Naushad, S. Shirazian, G. Walker and C. Mangwandi, *Chem. Eng. J.*, **307**, 264 (2017); https://doi.org/10.1016/j.cej.2016.08.089
93. P.N. Diagboya and E.D. Dikio, *J. Clean. Prod.*, **180**, 71 (2018); https://doi.org/10.1016/j.jclepro.2018.01.166
94. N.D. Shooto, *J. Environ. Chem. Eng.*, **8**, 104541 (2020); https://doi.org/10.1016/j.jece.2020.104541